from a filament consisting of a platinum plus 10 percent rhodium ribbon with a small tungsten ribbon spot-welded to it in a number of places. This arrangement was expected to give a film with the order of 10 percent excess barium.[6] The structure was not noticeably changed. An estimate of the minimum concentration of absorption centers associated with the peak at 3140A gives 0.03 percent while the value for the peak at 3200A would be considerably smaller.

The small widths of the major absorption peaks at half maximum (0.07 ev and 0.20 ev) and the fact that the structure sharpens with substrate temperature during evaporation of a film, appear to imply that the absorption is associated with the perfect lattice rather than with defects in the lattice. The sharpening of the structure at lower temperatures favors the view that these are exciton absorption peaks. Exciton absorption in BaO in the spectral region near 4.0 ev has been proposed to account for optical absorption and photoconductivity data,[7] photoemission,[8] and the temperature dependence of photoemission and photoconductivity.[9]

It should be noted that the absorption constant is at least as great as 300 cm^{-1} for single crystals of BaO prepared by a considerably different technique from these films,[5] and that the photoconductivity of these single crystals has a maximum in the region of the absorption peaks. Reflectivity measurements from single BaO crystals at low temperatures would be desirable to ascertain whether the density of these absorption centers is indeed as great in single crystals as it is in BaO films.

Overhauser[10] has pointed out that the observed structure can be understood in terms of an exciton model based on the tight binding approximation. The four absorption peaks arise from transitions between the ground state of the oxygen ion $(2p)^6$ and the four excited states of the $(2p)^5 3s$ configuration. The relative splittings of the four components can be fitted in terms of two constants: The exchange energy between $2p$ and $3s$ states and the spin-orbit splitting of the $(2p)^5$ ion core. A j-j coupling model is necessary. The absorption peaks at 3200A and 3140A are produced by transitions to excited states of angular momentum $J=0$ and 2, respectively. These peaks are weak because the transitions are forbidden by optical selection rules. The absorption peaks at 3050A and 2880A are produced by transitions to excited states for which $J=1$. They are allowed by optical selection rules and hence are strong.

The author is deeply indebted to Professor R. L. Sproull for his guidance and interest in this work and to Professors J. A. Krumhansl and A. W. Overhauser for discussions of interpretation.[11]

[6] Based on private communication from G. E. Moore.
[7] W. W. Tyler and R. L. Sproull, Phys. Rev. **83**, 548 (1951).
[8] Apker, Taft, and Dickey, Phys. Rev. **84**, 508 (1951).
[9] H. B. DeVore and J. W. Dewdney, Phys. Rev. **83**, 805 (1951).
[10] A. W. Overhauser (private communication).
[11] Since this work was performed, Mr. Koji Okumura has kindly communicated his studies of optical absorption of BaO films. He has found results similar to the 5°C curve of Fig. 3.

PHYSICAL REVIEW VOLUME 97, NUMBER 2 JANUARY 15, 1955

Dynamics of Simple Lattices*

HERBERT B. ROSENSTOCK
U. S. Naval Research Laboratory, Washington, D. C.
(Received June 15, 1954)

The critical points (points where $\partial\omega/\partial x_i=0$ for all $i=1,2,3$) of the frequency ω of the lattice vibrations in wave number space (x_1,x_2,x_3), shown by Van Hove to exist for a very general class of crystals, are located for the monatomic simple, face-centered, and body-centered cubic lattices. The position and nature of the resulting singularities in the frequency distribution are found as a function of the ratio of force constants for second-nearest neighbors and nearest neighbors, and the qualitative features of the frequency distribution are thus determined. A method for using the information so obtained to determine the frequency distribution quantitatively is outlined.

I. INTRODUCTION

THE general problem we are concerned with is the finding of the energy eigenvalues of the Schrödinger equation for a system consisting of a very large number of coupled harmonic oscillators arranged in space in a simple lattice. Physically this system is interpreted as a crystal, the oscillators as the constituent atoms. Since the number N of atoms and hence the number of eigenvalues in a macroscopic crystal is of the order of Avogadro's number, an actual numerical evaluation of the latter is impractical even after an analytical expression for them has been obtained; and we are faced with the additional, usually more difficult, problem of finding the distribution function $g(E)dE$ of energy levels, defined as the density

* Preliminary results reported at the Washington Meeting of the American Physical Society, April 1954 [Phys. Rev. **95**, 617 (1954)].

of energy levels to be found in the energy range $(E, E+dE)$. This function will determine the partition function $\int g(E)dE \exp(E/kT)$ and thus all other thermodynamic functions of the solid.[1] Among other fields in which frequency spectra are of interest may be mentioned optical properties (infrared absorption and Raman spectra), x-ray diffraction, superconductivity,[2] neutron scattering.[3]

Another way of formulating the problem, a semiclassical way, is to ask for the frequency eigenvalues ("normal modes") of the wave equation for the system described above considered classically, and for the "frequency distribution" $g(\omega^2)d\omega^2$, the fractional number of frequencies in the range $(\omega^2, \omega^2+d\omega^2)$, of them. The two formulations are equivalent mathematically, and also physically if Planck's assumption concerning the levels of an oscillator is made.[4] The semiclassical formulation is the one which is most used, even today, probably because the first paper on the subject[5] appeared before quantum mechanics was invented, and we shall generally follow this usage in this paper.

An exact calculation of the frequency spectrum has so far been possible for only very few crystals[6–14] (other than one-dimensional ones), and special, often physically unrealistic, assumptions had to be introduced. However, all frequency distributions found by exact calculation contained points of nonanalyticity: the two-dimensional crystals showed infinite logarithmic peaks, the three-dimensional ones infinite discontinuities in the slope. Van Hove[15] has traced the singularities to "critical points" (points where all $\partial\omega/\partial x_i=0$) of the surfaces of constant frequency in wave number space and has shown that a certain minimal number of critical points follows from the periodicity of ω in wave number space alone; hence that the frequency distribution of any crystal will show a minimum number of singularities.

In this paper we wish to show how the critical points, and from this the singularities in the frequency distribution, may be located for certain simple lattices. We use the square lattice first for an example in two dimensions and then treat the three-dimensional simple, face-centered, and body-centered cubic lattices. Finally we show how the information so obtained enables us to get a rather complete picture of the frequency distribution.

II. BACKGROUND AND NOTATION

We use the following abbreviations: CP for critical point(s), FD for frequency distribution, 1D, 2D, $\cdots i$D for one-dimensional, etc., sc, bcc, fcc for simple cubic, body-centered cubic, face-centered cubic.

The process of obtaining an expression for the frequencies of the normal modes of a monatomic lattice is straightforward and well known.[1] One sets the kinetic energy:

$$T=\tfrac{1}{2}m \sum_{\text{all } i,j,k} (\dot{u}_{ijk}^2+\dot{v}_{ijk}^2+\dot{w}_{ijk}^2),$$

and the potential energy:

$$V=[\tfrac{1}{2}\alpha \sum_{\substack{\text{nearest}\\ \text{neighbors}}} +\tfrac{1}{2}\beta \sum_{\substack{\text{2nd-nearest}\\ \text{neighbors}}}](d-d_0)^2.$$

Here $(u_{ijk},v_{ijk},w_{ijk})$ are the displacements in the (x,y,z) directions of the atom labeled according to its position by subscripts ijk. (If we are dealing with a 2D lattice the index k is not present.) d is the distance between two atoms and d_0 is the equilibrium distance; $d-d_0$ is to be expanded in the u, v, w and only the lowest nontrivial terms, leading to Hooke's law forces, are to be retained. m is the mass of each atom. α and β are force constants for nearest and second-nearest neighbors, respectively. One can then write down the Lagrangian equations of motion for each atom, solve these by standing waves with periodic boundary conditions, and thus obtain the secular equation:

$$\Delta(x_1,x_2,x_3;\alpha,\beta;\omega^2)=0, \tag{1}$$

which determines the squared frequency ω^2. Strictly speaking, $x_i=p_i\pi/N^{\frac{1}{3}}$ is defined only for integer values of p_i between $-N^{\frac{1}{3}}$ and $N^{\frac{1}{3}}$, but since N is a very large number, x_i may be considered as a continuous variable running from $-\pi$ to π. Let us write down the determinant Δ explicitly for the cases of interest, calling the diagonal elements f_{ii} and the offdiagonal ones f_{ij}. For the 2D square lattice, we have[6]

$$f_{ii}=(1-c_i)+\sigma(1-c_1c_2)-\lambda,$$
$$f_{ij}=\sigma(1-c_j^2); \tag{2}$$

[1] J. E. Mayer and M. G. Mayer, *Statistical Mechanics* (John Wiley and Sons, Inc., New York, 1940), Chap. XI.

[2] J. Bardeen, Phys. Rev. **80**, 567 (1950); H. Frohlich, Phys. Rev **79**, 845 (1950).

[3] G. Placzek and L. Van Hove, Phys. Rev. **93**, 1207 (1954).

[4] This equivalence follows essentially from the fact that semiclassical theory gives correct results when it deals with oscillators [see, e.g., L. Pauling and E. B. Wilson, *Quantum Mechanics* (McGraw-Hill Book Company, Inc., New York, 1935)], pp. 9, 30, 72. In connection with the problem at hand, this has been discussed explicitly by E. W. Montroll and D. C. Peaslee, J. Chem. Phys. **12**, 98 (1944), and it is brought up again only because conversations and the literature reveal that many persons seem to mistrust the results of the theory because it is usually formulated semiclassically. A remarkable example of this mistrust is the statement "*Die Schwingungen des idealen Gitters stellen ein quantenmechanisches System von makroskopischen Dimensionen dar; denn die Normalkoordinaten sind Amplituden von Wellen, die sich durch das ganze Gitter erstrecken. Das scheint eine bedenkliche Annahme.*" M. Born, *Festschrift Akademie der Wissenschaften, Gottingen* (Springer, Berlin, 1951), p. 1.

[5] M. Born and Th. von Kármán, Physik. Z. **13**, 297 (1912).

[6] E. W. Montroll, J. Chem. Phys. **15**, 575 (1947).

[7] M. Smollett, Proc. Phys. Soc. (London) **A65**, 109 (1952).

[8] W. A. Bowers and H. B. Rosenstock, J. Chem. Phys. **18**, 1056 (1950); **21**, 1607 (1953).

[9] G. F. Newell, J. Chem. Phys. **21**, 1877 (1953).

[10] C. M. Askey, thesis, University of North Carolina, Chapel Hill, North Carolina, 1951 (unpublished).

[11] J. P. Hobson and W. A. Nierenberg, Phys. Rev. **89**, 662 (1953).

[12] H. B. Rosenstock, J. Chem. Phys. **21**, 2064 (1953).

[13] H. B. Rosenstock and G. F. Newell, J. Chem. Phys. **21**, 1607 (1953).

[14] H. B. Rosenstock and H. M. Rosenstock, J. Chem. Phys. **21**, 1608 (1953).

[15] L. Van Hove, Phys. Rev. **89**, 1189 (1953).

for the 3D sc lattice, we have[14]

$$f_{ii}=(1-c_i)+\sigma(2-c_ic_j-c_ic_k)-\lambda,$$
$$f_{ij}=\sigma(1-c_j^2); \tag{3}$$

for the 3D bcc lattice, we have[16]

$$f_{ii}=1-c_1c_2c_3+\gamma(1-c_i^2)-\mu_3,$$
$$f_{ij}=(1-c_j^2)c_k; \tag{4}$$

for the 3D fcc lattice, we have[17]

$$f_{ii}=1-\tfrac{1}{2}c_i(c_j+c_k)+\sigma(1-c_i^2)-\mu_F$$
$$f_{ij}=\tfrac{1}{2}(1-c_j)^2. \tag{5}$$

Here $\sigma=\beta/\alpha$, $c_i=\cos x_i$, $\lambda=m\omega^2/2\alpha$, $\gamma=3\sigma/2$, $\mu_B=3\lambda/4$, $\mu_F=\lambda/2$ and the indices take on values 1, 2 in Eq. (2) and 1, 2, 3 in Eqs. (3), (4), and (5). Subscripts on μ_B and μ_F will be suppressed below.

We observe that in each case the secular equation (1) can be solved for λ or μ by elementary algebra, yielding three, or in the case of Eq. (2), two solutions ("branches") but that the expressions so obtained would be so complicated as to be of little use in finding the FD. Even the more restricted problem of finding the CP defined by $\partial\lambda/\partial x_i=0$ for all x_i is seen to present great algebraic difficulties when attacked by the straightforward approach of solving Eq. (1) for λ, differentiating with respect to x_1, x_2, x_3 and solving the resulting equations simultaneously. Henceforth, we shall therefore work mostly with the determinantal equation (1) itself rather than with the solutions which can in principle be explicitly obtained from it.

The first, and major problem of this paper, is to locate the CP of λ. Van Hove's paper,[15] in which the question of critical points and singularities in the frequency distribution caused by them was first generally treated, is based on a topological theorem due to Morse,[18] which van Hove states as follows:

> "Consider a function f defined on a closed topological manifold satisfying convenient conditions of differentiability and regularity. Assume f to be three times continuously differentiable and to have no degenerate critical points. Call index of a non-degenerate CP the number of positive eigenroots of the quadratic form in the Taylor expansion of f near the CP. Under these conditions the number of CP of index i is at least equal to the Betti number R_i of the manifold for the dimension i." By the Betti number R_i is meant "the maximum number of closed i-dimensional surfaces on the manifold which cannot be transformed into one another or into a point by a continuous deformation of the manifold." It is further stated that in two dimensions $R_0=1$, $R_1=2$, $R_2=1$, and in three dimensions $R_0=1$, $R_1=3$, $R_2=3$, $R_3=1$.

To the reader not versed in topology, it may not be clear from the above statement of the theorem, nor from the proof referred to,[18] that the predictions of the theorem for two- and three-dimensional spaces may also be obtained intuitively from extremely elementary considerations. Since in this paper more use is made of intuition than of mathematical rigor, a few words on this will be helpful.[19] Consider a function $f(x,y)$ periodic in both variables. (It helps to visualize this function as contour lines representing altitude, as on an ordinary geographical map.) Such a function is shown in Fig. 1. The unit cells of periodicity have without loss of generality been taken as squares and indicated in heavy lines. In the center cell, there will be at least one point where f takes on its maximum value[20]; we have called that point M and since in its neighborhood, the contours will be small closed curves, we have encircled it in Fig. 1a. From the required periodicity it follows that maxima will also appear at points labeled M_2, M_3, $\cdots$. Similarly, at least one minimum will exist in each cell, and these have been labeled m, m_1, m_2, $\cdots$ and also shown in Fig. 1a. Now consider the path of a traveler going from "mountain" M to "mountain" M_2 along some path A_1. He will have to start by going downhill, end up by going uphill, and reach a minimum somewhere in between, at a point which we may call (x_1,y_1). If he chooses an adjacent path A_2 instead, he will reach the minimum along that path at some adjacent point (x_2,y_2). Of all possible paths, there will exist one, A_i, at whose minimum the relation $f(x_i,y_i)>f(x_j,y_j)$ will be satisfied for all $j\neq i$. This point (x_i,y_i) is a saddle point and the contour is x-shaped there as indicated in Fig. 1b. In the same manner we see that another saddle point will appear between m and m_2. Other saddle points will appear at equivalent points in the other cells, by periodicity. In Fig. 1c these saddle points are shown connected up in the simplest possible way. We see that each cell has one maximum, one minimum and two saddle points; this is what Morse's theorem predicts for two dimensions. In three dimensions the surface $f=f_0$ through a saddle point is, near the saddle point, shaped like a double cone; adjacent surfaces are hyperboloids of one sheet for $f\lesseqgtr f_0$ and hyperboloids of two sheets for $f\gtreqless f_0$ and the saddle point is called an $S_\pm$ point accordingly. The reader who will construct (or visualize) the 3D model corresponding to Fig. 1 will have no difficulty convincing himself, by the same type of argument as we used for two dimensions, that each periodicity cell will con-

[16] P. C. Fine, Phys. Rev. **56**, 355 (1939).
[17] R. B. Leighton, Revs. Modern Phys. **20**, 165 (1948).
[18] M. Morse, Am. Math. Monthly **49**, 358 (1952); Trans. Am. Math. Soc. **27**, 345 (1925).
[19] A very similar "heuristic discussion" of Morse's theorem is given by E. W. Montroll, Am. Math. Monthly **61**, No. 7 (suppl), 46 (1954).
[20] The situation where the maximum value is taken on by a continuous family of points (a curve) can arise, but may be regarded as exceptional.

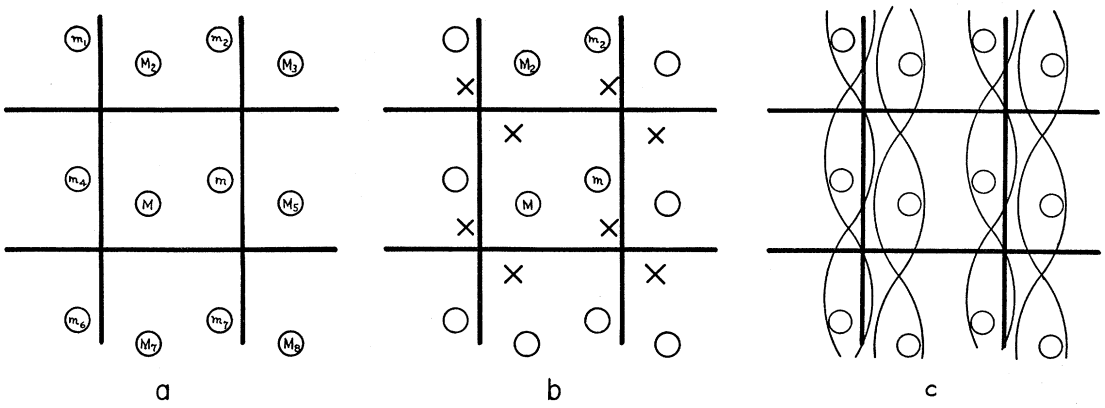

FIG. 1. Illustration of the predictions of Morse's theorem in two dimensions. Detailed explanation in text, Sec. II.

tain at least one maximum, one minimum, three S_+ points and three S_- points, in agreement with Morse's theorem.

Finally we wish to review briefly the conclusions of Van Hove concerning the nature of the singularities in the frequency distribution which each of the above CP will cause in a 3D crystal. This is done in Table I. Table I will enable us to sketch the frequency distribution as soon as we have located all the CP. Care must be exercised only in eliminating "generalized" CP which might give rise to less strong singularities.[21]

III. LOCATING THE CRITICAL POINTS

We have seen in the preceding section that we cannot hope to find the critical points by straightforwardly solving the three equations $\partial\lambda/\partial x_i=0$ simultaneously. In looking for another method we observe that λ as given by (1) with (2), (3), (4), or (5) depends on the x_i only through the $c_i=\cos x_i$. It follows first of all that we may restrict ourselves to considering the half-periodicity cube, $0\leq x_1, x_2 x_3\leq\pi$. Furthermore we may write $\partial\lambda/\partial x_i=(dc_i/dx_i)(\partial\lambda/\partial c_i)=-\sin x_i(\partial\lambda/\partial c_i)$. Since therefore $\partial\lambda/\partial x_i=0$ if and only if either $\sin x_i=0$ or[22] $\partial\lambda/\partial c_i=0$ it follows that we may have the following types of CP:

Type-1 CP All three $\sin x_i$ vanish.
Type-2 CP Two $\sin x_i$ vanish and one $\partial\lambda/\partial c_i$ vanishes.
Type-3 CP One $\sin x_i$ vanishes and two $\partial\lambda/\partial c_i$ vanish.
Type-4 CP All three $\partial\lambda/\partial c_i$ vanish.

[21] "Generalized critical points" are defined in reference 15 as points near which the topological shape of the surfaces is the same as for ordinary CP but at which the equations $\partial\lambda/\partial x_i=0$ do not hold. The generalized critical point that appears in reference 15 at the absolute minimum of frequencies appears as an ordinary CP in our paper because we consider the distribution of $\lambda=m\omega^2/2\alpha$ rather than ω as does Van Hove. Since it is λ rather than ω that appears in the secular equation, this leads to other simplifications as well. Transition from the distribution $g(\lambda)d\lambda$ of λ to the distribution $G(\omega)d\omega$ of ω is made by noting that we must have $g(\lambda)d\lambda=G(\omega)d\omega$; hence $g(\lambda)[m/2\alpha]2\omega d\omega=G(\omega)d\omega$ or $G(\omega)=m\omega g(\lambda)/\alpha$.

[22] A possible exception to this statement might arise if $\partial\lambda/\partial c_i=\infty$ at a point at which $\sin x_i=0$. This does not occur.

Now $\sin x_i$ vanishes only when x_i is 0 or π. Since in the above classification no other mention appears of the x_i, we may henceforth consider the c_i as our variables and pay no more attention to the x_i. Henceforth when we speak of corners, faces, or other features of a cube, we shall mean the cube $-1\leq c_1, c_2, c_3\leq 1$. We may now say:

Type-1 CP appear at the 8 corners.
Type-2 CP appear on edges, at (1D) minima or maxima along the edges.
Type-3 CP appear on faces, at (2D) maxima, minima, or saddle points on the faces.
Type-4 CP appear inside the cube.

We have thus already located the minimum number 8 of CP predicted by Morse's theorem (the 8 Type-1 CP at the 8 corners). This of course is no accident but rather a consequence of the fact that Morse's theorem is arrived at entirely by periodicity considerations, and that the Type-1 CP are the ones that owe existence entirely to periodicity. The other type CP also depend to a greater or lesser extent on the detailed structure of the secular equation and are correspondingly harder to locate.

The locating of Type-2 CP is still rather easy. When two $\sin x_i$ vanish, four off-diagonal terms vanish, the determinant factors into the three diagonal terms which are linear in λ, and each of these can be considered individually. Each contains only one variable in which it is at most quadratic, the equation $\partial\lambda/\partial c_i=0$ is therefore easily solved, and the Type-2 CP have been found.

TABLE I. Nature of singularities in the frequency distribution (FD) of a three-dimensional (3D) crystal caused by ordinary (not generalized) critical points (CP). Here $\epsilon>0$; the table gives the first nonconstant term in the expansion of $g(\lambda)$ about λ_c; $\pm$ indicates the sign of the term's coefficient.

CP at λ_0	$g(\lambda_c-\epsilon)$	$g(\lambda_c+\epsilon)$
maximum M	$+\epsilon^{\frac{1}{2}}$	ϵ
minimum m	ϵ	$+\epsilon^{\frac{1}{2}}$
saddle point S_-	$-\epsilon^{\frac{1}{2}}$	ϵ
saddle point S_+	ϵ	$-\epsilon^{\frac{1}{2}}$

The method for locating Type-3 CP, the ones that appear on a plane (square) is best explained by using the square lattice, Eqs. (1), (2), as an example. The equation is quadratic, so there will be two solutions; but, as explained in Sec. 2, we wish to avoid considering these in detail as their form will be rather complicated. However, their behavior on the edges is simpler and is easily found by equating c_1 or c_2 to 1 or -1; this causes the determinant to factor into two terms linear in λ. (If the Type-2 CP have been found explicitly, then this work has already been done.) We thus get:

$$\begin{aligned}
&\text{when } c_1=1,\ \begin{cases}\lambda_1=\sigma(1-c_2) & \text{from the } f_{11} \text{ term,}\\ \lambda_2=(1+\sigma)(1-c_2) & \text{from the } f_{22} \text{ term;}\end{cases}\\
&\text{when } c_2=1,\ \begin{cases}\lambda_3=(1+\sigma)(1-c_1) & \text{from the } f_{11} \text{ term,}\\ \lambda_4=\sigma(1-c_1) & \text{from the } f_{22} \text{ term;}\end{cases}
\end{aligned} \tag{6}$$

and similar expressions when c_1 or c_2 are -1. In this way we determine the behavior of λ on the boundary of the square, and from this we shall attempt to find its behavior inside the square. One question which arises first however is whether at $(c_1,c_2)=(1,1)$ we shall join λ_1 to λ_3 and λ_2 to λ_4 or λ_1 to λ_4 and λ_2 to λ_3. (All four solutions take on the value of 0 at that point, so that at first sight either choice would seem possible. Points where two solutions take on the same value are called "contacts between branches" by Van Hove.[15]) In two dimensions this question can be easily and explicitly resolved. Consider the equation

$$\begin{vmatrix} A-\lambda & C \\ D & B-\lambda \end{vmatrix}=0. \tag{7}$$

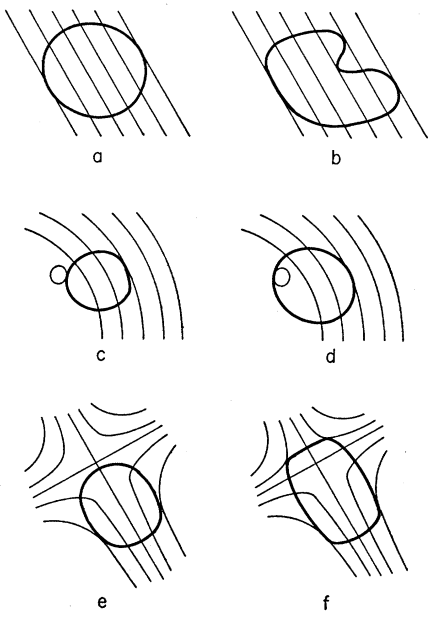

FIG. 2. Illustration of the relation between M_1 points on the boundary of a region and the two-dimensional critical points inside it. Detailed explanation in text, Sec. III.

Its two solutions are

$$\begin{aligned}
2\lambda_+&=A+B+[(A-B)^2+4CD]^{\frac{1}{2}},\\
2\lambda_-&=A+B-[(A-B)^2+4CD]^{\frac{1}{2}},
\end{aligned} \tag{8}$$

where we wish to emphasize that, as usual, $[\ ]^{\frac{1}{2}}$ means the positive square root. If A, B, C, D are functions of two parameters x, y, note that $\lambda_+\geq\lambda_-$ for all x, y. When CD approaches 0, (8) approaches

$$\begin{aligned}
2\lambda_+&=A+B+|A-B|,\\
2\lambda_-&=A+B-|A-B|,
\end{aligned}$$

or

$$\begin{aligned}
\lambda_+&=A \text{ or } B, \text{ whichever is larger,}\\
\lambda_-&=A \text{ or } B, \text{ whichever is smaller.}
\end{aligned} \tag{9}$$

This makes it clear that in (6) we must join λ_1 to λ_4 and λ_2 to λ_3. Observe that simply joining the solution arising from the f_{11} term for $c_1=1$ to the solution arising from the f_{11} term for $c_2=1$ would have been incorrect.

More generally we may assert: in order to properly identify solutions, it is sufficient to make sure that if $\lambda_1\leq\lambda_2\leq\lambda_3$ at any one point, then $\lambda_1\leq\lambda_2\leq\lambda_3$ at all points. For if, for any two points, there exists a path along which λ_1 is never equal λ_2, then λ_1 will be the larger at the end point if it started out larger at the initial point, and our rule for identification becomes necessary as well as sufficient; whereas if no such path connecting the two points exists, the two points must be separated by a continuous curve (or, in three dimensions, by a continuous surface) of points where the two solutions are equal; so that it then does not matter how the identification is made. Thus sufficiency is assured in either case. This argument and conclusion is equally valid in two or three dimensions; we shall have to keep it in mind also for locating Type-4 CP later.

We have now established the behavior of the solutions on the edges which bound the faces; in particular we know (from the work for Type-2 CP) the 1D maxima and minima along the bounding edges. We shall now show how this gives us considerable information concerning the 2D maxima, minima and saddle points in the square inside those edges. In Fig. 2, the heavy lines represent a closed curve bounding a region, and light lines, as before, are contours of constant frequency. (Although in most cases that concern us here, the region is a square, we have not drawn it so in order to emphasize the greater generality of the argument.) In Fig. 2a, no 2D CP is enclosed, and we find one 1D minimum and one 1D maximum along the boundary. This is the simplest possible case. In Fig. 2b, the boundary (or the contours or both) have been distorted and as a result four M_1 points now appear on the boundary (notation: and M_i point is an iD maximum or minimum). Note that at three M_1 points, the contours are tangent to the boundary from the outside (we call them $M_1{}^o$ points); and at one M_1 point, the contour is tangent to the

TABLE II. Possible 2D CP inside a region along whose boundary the 1D maxima and minima are known.

$M_1^o-M_1^i$	S_2-M_2	S_2	M_2	Illustration
−2	−2	0	2	Fig. 3a
		1	3	
		2	4	
		etc.		
0	−1	0	1	Fig. 3b
		1	2	
		2	3	
		etc.		
2	0	0	0	Fig. 3c
		1	1	Fig. 3d
		2	2	
		etc.		
4	1	1	0	Fig. 3e
		2	1	Fig. 3f
		3	2	
		etc.		
6	2	2	0	Fig. 3g
		3	1	
		4	2	
		etc.		
etc.				

boundary from the inside (we call this an M_1^i point). We can convince ourselves that by distorting the contours or the boundary, we can add M_1^i points and M_1^o points only in pairs, and that $M_1^o-M_1^i$ will remain equal to 2 under such distortions. Now assume that in a simple configuration as in Fig. 2a, a M_2 point is just outside the boundary (Fig. 2c) and observe what happens if the boundary is slightly distorted so that the M_2 point gets into the bounded region (Fig. 2d). We see that the result is the addition of one M_1^i point to the boundary and the removal of one M_1^o point from it. Similarly, Fig. 2e and 2f shows what happens to the boundary if it is distorted so as to enclose a new S_2 point (a two-dimensional saddle point); two M_1^o points get added to the boundary. We may summarize the results by writing

$$M_1^o-M_1^i=2+2S_2-2M_2. \tag{10}$$

This may be solved to give

$$S_2-M_2=\tfrac{1}{2}(M_1^o-M_1^i)-1. \tag{11}$$

From Eq. (11), Table II may be constructed. Table II tells what configurations of M_2 and S_2 points we may expect if we know the M_1^o and M_1^i, points on the boundary. (It should be added that in practice M_1^o and M_1^i points are readily distinguished by expanding the secular equation about them.) Some of the possibilities of Table II are illustrated in Fig. 3. For each value of $M_1^o-M_1^i$, an infinite number of possible configurations still remain, to be sure, but for the simple lattices we consider here and for comparatively low values of the force-constant ratio σ, only the simpler ones occur, and symmetry considerations enable us to decide which. Take, e.g., the square lattice again: λ as defined there is symmetrical about the line $c_1=c_2$, and it follows from this that if any S_2 or M_2 are contained in the square at all, at least one of them will appear on that line. A CP located on this diagonal is again easily found and investigated on account of the fact that the determinant simplifies along it. Detailed calculations are given in the next section.

The same general ideas that enables us to locate the Type-3 CP on the faces also apply to locating the Type-4 CP inside the cube. Although we have not been able to formalize our work by establishing a rule like (11), the study of two-dimensional M_2 or S_2 points on the surface of the cube, together with symmetry considerations, enable us, as is shown in the next section, to locate the fortunately small number of Type-4 CP that the lattices of interest show for fairly small σ.

IV. LOCATING THE CRITICAL POINTS—CALCULATIONS

A. Square Lattice

It is convenient to write

$$\begin{aligned}\bar{\mu}&=\lambda/(1+\sigma),\\ \tau&=\sigma/(1+\sigma),\\ p&=1-c_1,\\ q&=1-c_2,\end{aligned} \tag{12}$$

and to consider the square $0<p,\ q<2$ for $0<\tau<1$. The secular equation (1) with (2) beomes then

$$0=\Delta_2(p,q;\tau;\bar{\mu})$$
$$\equiv\begin{vmatrix} p+\tau q(1-p)-\bar{\mu} & \tau q(2-q) \\ \tau p(2-p) & q+\tau p(1-q)-\bar{\mu}\end{vmatrix}. \tag{13}$$

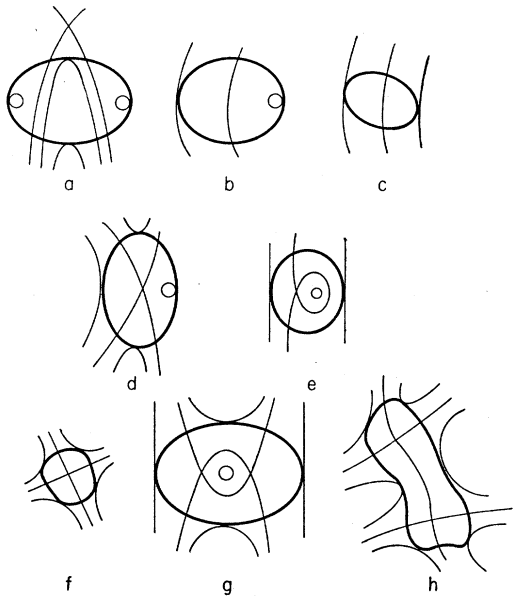

FIG. 3. Illustration of some of the configurations derived in Table II.

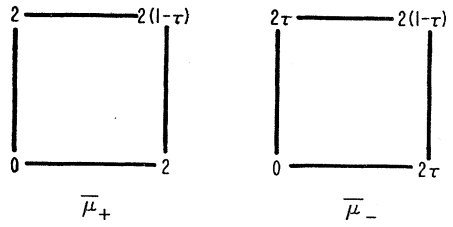

FIG. 4. Behavior of the solutions for the square lattice along the edges. Numbers show the values taken on by the two solutions at the corners.

Along the edge $p=0$ this reduces to

$$\bar{\mu}_1=\tau q, \quad \bar{\mu}_2=q; \tag{14a}$$

and along the edge $p=2$ this reduces to

$$\bar{\mu}_3=2-\tau q, \quad \bar{\mu}_4=2\tau+(1-2\tau)q, \tag{14b}$$

with similar expressions for the edges $q=0$, 2. Since the expressions (14) are linear, there will be no minima or maxima along the edges except possibly the end points (corners). Which solution is to be joined to which at the corners is determined by continuity at (0,2) and (2,0) and by the rule established in Sec. III at (0,0) and (2,2). Figure 4 shows the result. We see that $\bar{\mu}_+$ has along its boundary two minima at (0,0) and (2,2), and two maxima, at (0,2) and (2,0); $\bar{\mu}_-$ has along its boundary one minimum at (0,0) and one maximum at (2,2) if $\tau<\frac{1}{2}$, but has the same location of maxima and minima as $\bar{\mu}_+$ if $\tau>\frac{1}{2}$. To determine whether these are M_1^o or M_1^i points, we expand (13) about them and find: (0,0) is an M_1^o point in both $\bar{\mu}_+$ and $\bar{\mu}_-$ for all τ. (0,2) and (2,0) are M_1^o points for $\bar{\mu}_+$ for all τ, and M_1^o points for $\bar{\mu}_-$ for $\tau>\frac{1}{2}$. For $\bar{\mu}_+$, (2,2) is an M_1^i point for $\tau<\frac{1}{5}$ and an M_1^o point for $\tau>\frac{1}{5}$; for $\bar{\mu}_-$ it is an M_1^o point for $\tau<\frac{1}{2}$ and an M_1^i point for $\tau>\frac{1}{2}$. All this is illustrated in Fig. 5.

Next we look for 2D CP along the main diagonal (see the remark near the end of Sec. III) by setting $p=q$ and finding maxima or minima along that line by differentiation. We find only one, $\bar{\mu}=(1+3\tau)^2/8\tau$ located at $p=q=(1+3\tau)/4\tau$. This point is located inside the square for $\tau>\frac{1}{5}$, belongs to $\bar{\mu}_+$, and by expanding about it we find that it is a saddle point when $\tau>\frac{1}{5}$. Table II now tells us unambiguously that for $\bar{\mu}_-$, $(S_2,M_2)=(0,0)$ for all τ, and that for $\bar{\mu}_+$, $(S_2,M_2)=(0,0)$ for $\tau>\frac{1}{5}$. For $\bar{\mu}_+$ with $\tau>\frac{1}{5}$ there remain only the possibilities $(S_2,M_2)=(1,0)$, (3,2), (5,4), etc., since if there were an odd number of M_2, symmetry would demand that at least one of them show up on the main diagonal, and we reject all but (1,0) as too complicated to result from (13). The final sketches, Fig. 6, showing all CP, may now be made. We see that only three topological configurations occur; we shall call them L, M, N as defined in Table III.

B. Simple Cubic Lattice

It is convenient to write

$$\mu=\lambda/(1+2\sigma), \quad \rho=\sigma/(1+2\sigma),$$
$$p=1-c_1, \quad q=1-c_2, \quad r=1-c_3, \tag{15}$$

and to consider the cube $0<p,q,r<2$ for $0<\rho<1$. (1) with (3) then become

$$0=\begin{vmatrix} p+\rho(q+r)(1-p)-\mu & \rho q(2-q) & \rho r(2-r) \\ \rho p(2-p) & q+\rho(p+r)(1-q)-\mu & \rho r(2-r) \\ \rho p(2-p) & \rho q(2-q) & r+\rho(p+q)(1-r)-\mu \end{vmatrix}. \tag{16}$$

The behavior along the edges is established by equating two of the variables p, q, r to 0 or 2. Again we find that along each edge μ is linear in the third variable. From the symmetry of the determinant together with the rule for joining given in Sec. III, it follows that the cube surface of each of the three solutions of (16) will consist of two sets of three identical faces. The behavior on one set of these faces is found by setting one of the three variables equal to 0, on the other set by setting one of the variables equal to 2. Upon setting $r=0$, (16) gives

$$[\rho(p+q)-\mu]\Delta_2(p,q;\rho;\mu)=0, \tag{17}$$

TABLE III. Notation concerning configurations exhibited in Fig. 6 for the square lattice.

Range of τ	Configuration of $\bar{\mu}_+(\tau)$	Configuration of $\bar{\mu}_-(\tau)$
$0<\tau<\frac{1}{5}$	L	N
$\frac{1}{5}<\tau<\frac{1}{2}$	M	N
$\frac{1}{2}<\tau<1$	M	L

where Δ_2 is defined by (13) and analyzed in Sec. IVA. Upon setting $r=2$, (16) gives

$$[2-\rho(p+q)-\mu]\Delta_2(p,q;\sigma;\nu)=0, \tag{18}$$

with σ related to ρ by (15) and $\nu=(\mu-2\rho)/(1-2\rho)$. The cube faces are thus completely determined by the work of Sec. IVA and the simple expressions in the brackets of Eqs. (17), (18). After joining them up properly we find for the faces of the three solutions:

$$\mu_1(\rho)=\begin{cases}\rho(p+q) & \text{on front faces,}\\ (1-2\rho)\bar{\mu}_-(\sigma)+2\rho & \text{on back faces;}\end{cases}$$
$$\mu_2(\rho)=\begin{cases}\bar{\mu}_-(\rho) & \text{on front faces,}\\ (1-2\rho)\bar{\mu}_+(\sigma)+2\rho & \text{on back faces;}\end{cases} \tag{19}$$
$$\mu_3(\rho)=\begin{cases}\bar{\mu}_+(\rho) & \text{on front faces,}\\ 2-\rho(p+q) & \text{on back faces.}\end{cases}$$

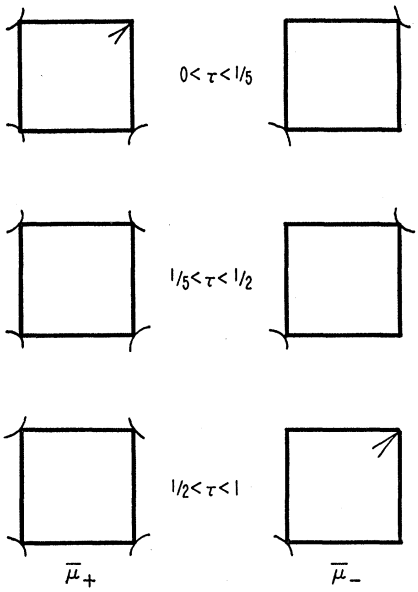

FIG. 5. M_1^i and M_1^o points for the square lattice.

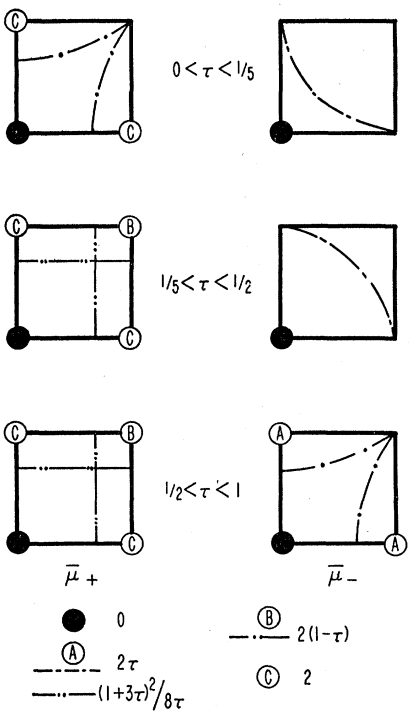

FIG. 6. Sketches of curves of constant frequency, square lattice.

Here $\bar{\mu}_\pm(\tau)$ are the functions sketched in Fig. 6; by "front" and "back" faces, we mean faces containing points $(p,q,r)=(0,0,0)$ and $(2,2,2)$, respectively. The two variables not constant on a face have for simplicity been written p, q. We may now use Table III to prepare an analogous table (Table IV) for the faces of the cube and also sketches of the surfaces (contained in Fig. 7). All Type-1 and Type-3 CP can be read off the sketches; there are no Type-2 CP. To locate the Type-4 CP we investigate the main diagonal of the cube and find one CP, $\mu_5=(1+6\rho)^2/16\rho$ located at $p=(1+6\rho)/8\rho$, and a double one, $\mu_6=1/4\rho$ located at $p=1/2\rho$. μ_5 is inside the cube if $\rho>1/10$, and by expanding we find that it is an S_3 point for $1/10<\rho<(2\sqrt{10}-5)/6\cong 0.221$ and an M_3 point otherwise. When it is an M_3 point the configuration becomes much more complicated and we shall therefore restrict ourselves to $\rho<0.221$ henceforth. This stipulation also eliminates all consideration of the CP μ_6, as it is inside the cube only when $\rho>\frac{1}{4}$. Study of the surfaces in Fig. 7 shows that the entry of an S_3 point into the cube at $\rho=1/10$ at the point (2,2,2) is possible without change in the surface configuration only for the solution μ_3. Finally we remark that when $\rho=0$ we get two-dimensional continua[23] of critical points at the frequencies 0, 2. We are now able to exhibit in Fig. 7 sketches showing all critical surfaces for all ρ from 0 to 0.221.[24] The CP are listed in Table V.

TABLE IV. Configurations on curbe faces for simple cubic (sc) lattice, as exhibited in Fig. 7. Notation as in Table III.

Range of σ	Range of ρ	Configuration of $\mu_3(\rho)$ front face	$\mu_3(\rho)$ back face	$\mu_2(\rho)$ front face	$\mu_2(\rho)$ back face	$\mu_1(\rho)$ front face	$\mu_1(\rho)$ back face
$0<\sigma<\frac{1}{5}$	$0<\rho<\frac{1}{7}$	N	N	N	L	L	N
$\frac{1}{5}<\sigma<\frac{1}{3}$	$\frac{1}{7}<\rho<\frac{1}{5}$	N	N	N	M	L	N
$\frac{1}{3}<\sigma<\frac{1}{2}$	$\frac{1}{5}<\rho<\frac{1}{4}$	N	N	N	M	M	N

C. Body-Centered Cubic Lattice

This is more conveniently treated in terms of the original c_i rather than the p, q, r. One solution is found not to be linear along the edges, but no maximum or

TABLE V. Critical frequencies for the simple cubic lattice.

μ	CP		Range
0	m		all
$\mu_1=2\rho$	S_-		all
$\mu_2=4\rho$	S_+		all
$\mu_3=2-4\rho$	S_-		all
$\mu_4=2-2\rho$	S_+		all
$\mu_{\max}=2$	M		all
$\mu_5=(1+6\rho)^2/16\rho$	S_-	$\frac{1}{10}<\rho<0.221$	$\rho>\frac{1}{10}$
	M	$0.221<\rho$	
$\mu_7=(1+3\rho)^2/8\rho$	S_+		$\rho>\frac{1}{5}$
$\mu_8=2\rho+(1+\rho)^2/8\rho$	S_+		$\rho>\frac{1}{7}$

[23] This, and its effect on the frequency spectrum (see Sec. V) is well known. See, e.g., the discussion by Newell, reference 9. Newell has also predicted the entry into the cube of the S_3 point μ_5 when $\rho=1/10$.

[24] To the reader who has difficulty visualizing the connectedness of the surfaces from the rather congested drawing of Fig. 7, we suggest that he first prepare cubes (or half-cubes respectively) and drawn the appropriate lines on the surfaces; and that he then redraw the same figures on a sphere (or hemisphere respectively) or similar figure containing no sharp edges or corners to confuse him.

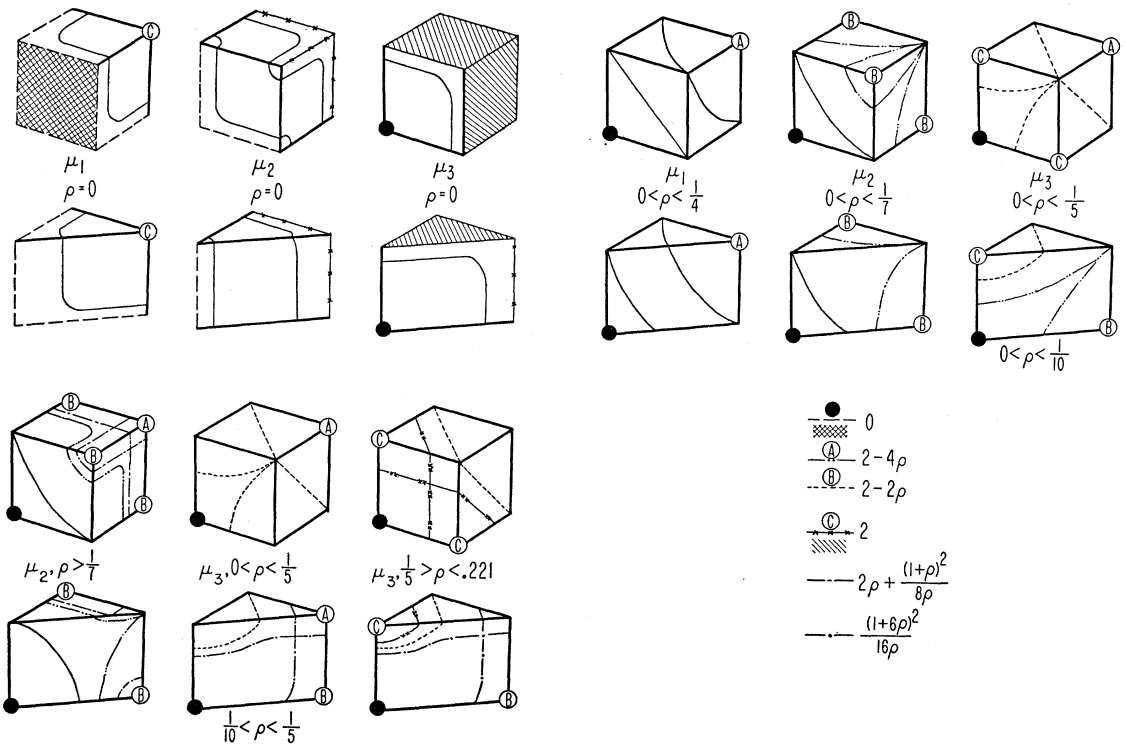

FIG. 7. Sketches of surfaces of constant frequency, simple cubic lattice.

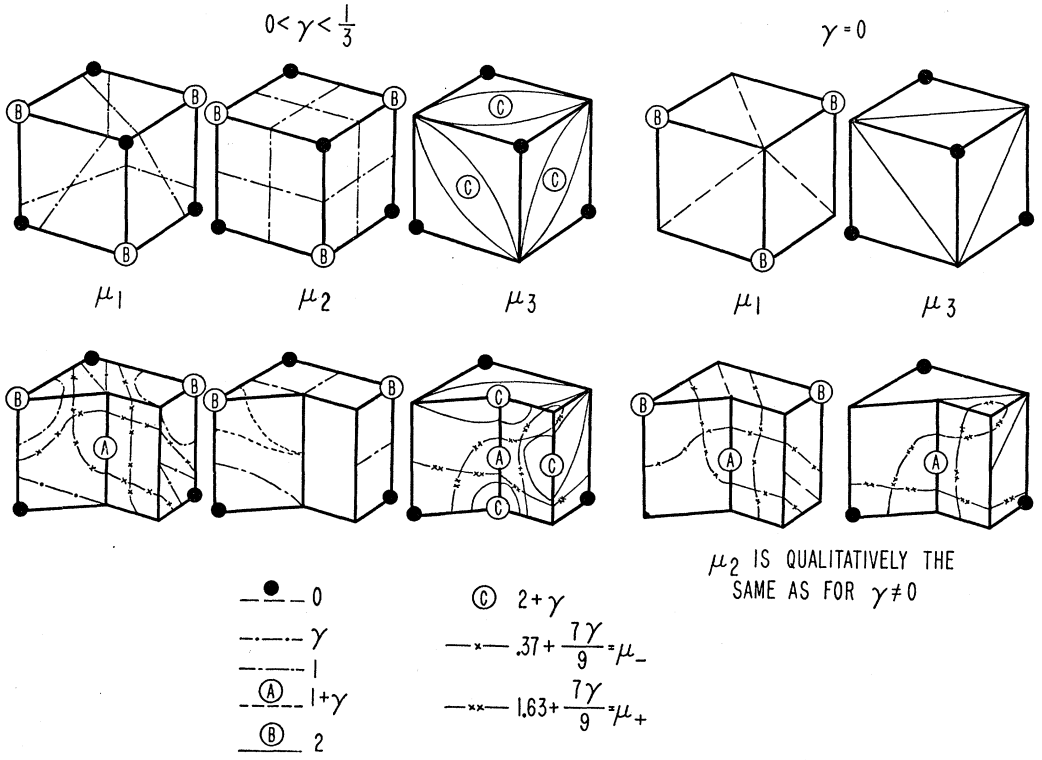

FIG. 8. Sketches of surfaces of constant frequency, body-centered cubic lattice.

minimum occurs for $-1<c_i<1$ unless $\gamma>\frac{1}{2}$; if we therefore take $\gamma<\frac{1}{2}$ there will be again no Type-2 CP. To find the behavior on the faces we again set $c_3=1$ for the front face and get

$$[1-c_1c_2-\lambda]\Delta_B(c_1,c_2;\gamma;\mu)=0, \qquad (20)$$

Δ_B being what is left of the 2×2 determinant formed by f_{11}, f_{12}, f_{21}, f_{22}. For the back faces we set $c_1=-1$ and find

$$[1+c_1c_2-\lambda]\Delta_B(c_1,-c_2;\gamma;\mu)=0. \qquad (21)$$

This shows that this time all six faces are alike except for a 90° rotation. If the two solutions arising from Δ_B in (20) or (21) are considered separately from the one arising from the bracket, it is found that the sufficient condition for joining (Sec. III) is satisfied and that in order to satisfy the convention that $\mu_1\leq\mu_2\leq\mu_3$ everywhere, the solution arising from the bracket should be labeled μ_2. The CP on the faces are found by the by now familiar method of first finding the nature of the M_1 points on the edges and then along the main face diagonal; each face is found to have one CP at $(c_i,c_j)=(0,0)$ as shown on the sketches on Fig. 8. Inside the cube along the main diagonal we find first of all critical points at $c_1=c_2=c_3=[-\gamma\pm(\gamma^2+18)^{\frac{1}{2}}]/9\cong\pm\sqrt{2}/3-\gamma/9$ where $\mu=2-2\gamma c_1-9\gamma c_1^2\cong1\pm0.63+7\gamma/9$, which upon expansion turn out to be saddle points for small σ. By symmetry, all diagonals are equivalent and hence the same saddle points appear on all of them. As we pass through the origin along the main diagonal, the first derivative does not vanish for any solution but the second derivative does; all solutions become equal there and in order to preserve the relations $\mu_1\leq\mu_2\leq\mu_3$ it is necessary to rearrange them properly. Even though the generalized CP resulting from this rearrangement will not cause a "strong" singularity (no discontinuity in the slope but only in the second derivative) in the FD, we must nonetheless study them carefully in order to determine the possible shapes of the surfaces throughout the cube. By expanding the original determinant about $(c_1,c_2,c_3)=(0,0,0)$, the solutions appear in the proper way directly. We thus find that μ_3 has a minimum, μ_1 a maximum, and μ_2 a double saddle point [the shape of the surface of μ_2 through (0,0,0) near (0,0,0) is a quadruple cone, the axis pointing to the points $(1,1,-1)(1,-1,1)$, $(-1,1,1)$, $(-1,-1,-1)$]. It turns out that these are all the critical points needed to give a consistent picture of all surfaces. They are shown in Fig. 8,[25] and listed in Table VI.

D. Face-Centered Cubic Lattice

The larger number of points- and line-contacts between branches makes the study of this lattice substantially more involved than of the preceding ones. Again we begin by investigating μ along the edges; then, upon considering the front faces $c_3=1$, we get

$$[2-(c_1+c_2)-\mu]\Delta_F(c_1,c_2;\sigma;\mu)=0, \qquad (22)$$

with Δ_F defined in analogy with (20). At the back faces $c_3=1$, we get

$$[2+(c_1+c_2)-\mu]\Delta_F(-c_1,-c_2;\sigma,\mu)=0, \qquad (23)$$

and so again only one face need be studied in detail. The one CP on the main diagonal of the face, at $c_1=c_2=(5+4\sigma)/4(1+\sigma)$ where $\mu=(5+4\sigma)^2/16(1+\sigma)$, is found to be an S_2 point for $\sigma<\sigma^+\cong0.149$ and an M_2 point for $\sigma>\sigma^+$. [Precisely, σ^+ is defined as the solution of the equation $\sigma(5+4\sigma)(3+4\sigma)=3$.] The generalized CP $(3+4\sigma)/(2+2\sigma)$ and $\frac{3}{2}$ result from interchanging solutions along the line contact running from $(-1,0)$ to $(0,-1)$ on each face. The configuration on the surface changes when at $\sigma=0$ these two frequencies become equal and again when at $\sigma=(-2+\sqrt{3})/4\cong-0.067$ when $(5+4\sigma)^2/16(1+\sigma)$ and $\frac{3}{2}$ become equal. These changes do not seem to affect the structure of the surfaces inside the cube qualitatively, however. After ascertaining the behavior of the solutions at the corners and other M_1 points on the edges, the configurations

TABLE VI. Critical frequencies for the body-centered cubic (bcc) lattice. Good to $\gamma=\frac{1}{3}$. When $\gamma=0$, 0 and γ coalesce, and 2 and $2+\gamma$ coalesce to give a continuous line of CP.

μ	CP
0	m
γ	S_-
$\mu_-\cong0.37+7\gamma/9$	S_+
1	S_-
$1+\gamma$	(S,M,m)(generalized)
$\mu_+\cong1.63+7\gamma/9$	S_-
2	S_+,M,M
$2+\gamma$	M

TABLE VII. Critical frequencies for the face-centered cubic (fcc) lattice. Only ordinary (not generalized) CP are shown.

σ	μ	CP
$-\frac{1}{4}<\sigma<-0.067$	0	m
	$\frac{1}{2}+\sigma$	S_-
	$1+\sigma$	S_+
	1	M,S_-
	$(5+4\sigma)^2/16(1+\sigma)$	M
	$\mu^*\cong1.8$	S_+
	$2+\sigma$	M
	2	M
$-0.067<\sigma<0$	$(5+4\sigma)^2/16(1+\sigma)$	S_+
	otherwise unchanged	
$\sigma=0$	1 and $1+\sigma$ coalesce to give a continuous line CP	
	2 and $2+\sigma$ coalesce	
$0<\sigma<0.149$	0	m
	$\frac{1}{2}+\sigma$	S_-
	1	S_-,S_+
	$1+\sigma$	M
	$(5+4\sigma)^2/16(1+\sigma)$	S_+
	$\mu^*\cong1.8$	S_+
	2	M
	$2+\sigma$	M

[25] The surfaces are seen to be more complicated than in Fig. 7. The essentials of μ_2 have been described in the text. μ_1 may be visualized best by paying most attention to the surface $\mu=0.37+7\sigma/9$. It consists of one closed surface which encloses the center of the cube and which touches, at four points located on the diagonals, four cup-shaped surfaces each of which surrounds one corner of the cube. μ_3 has a similar structure.

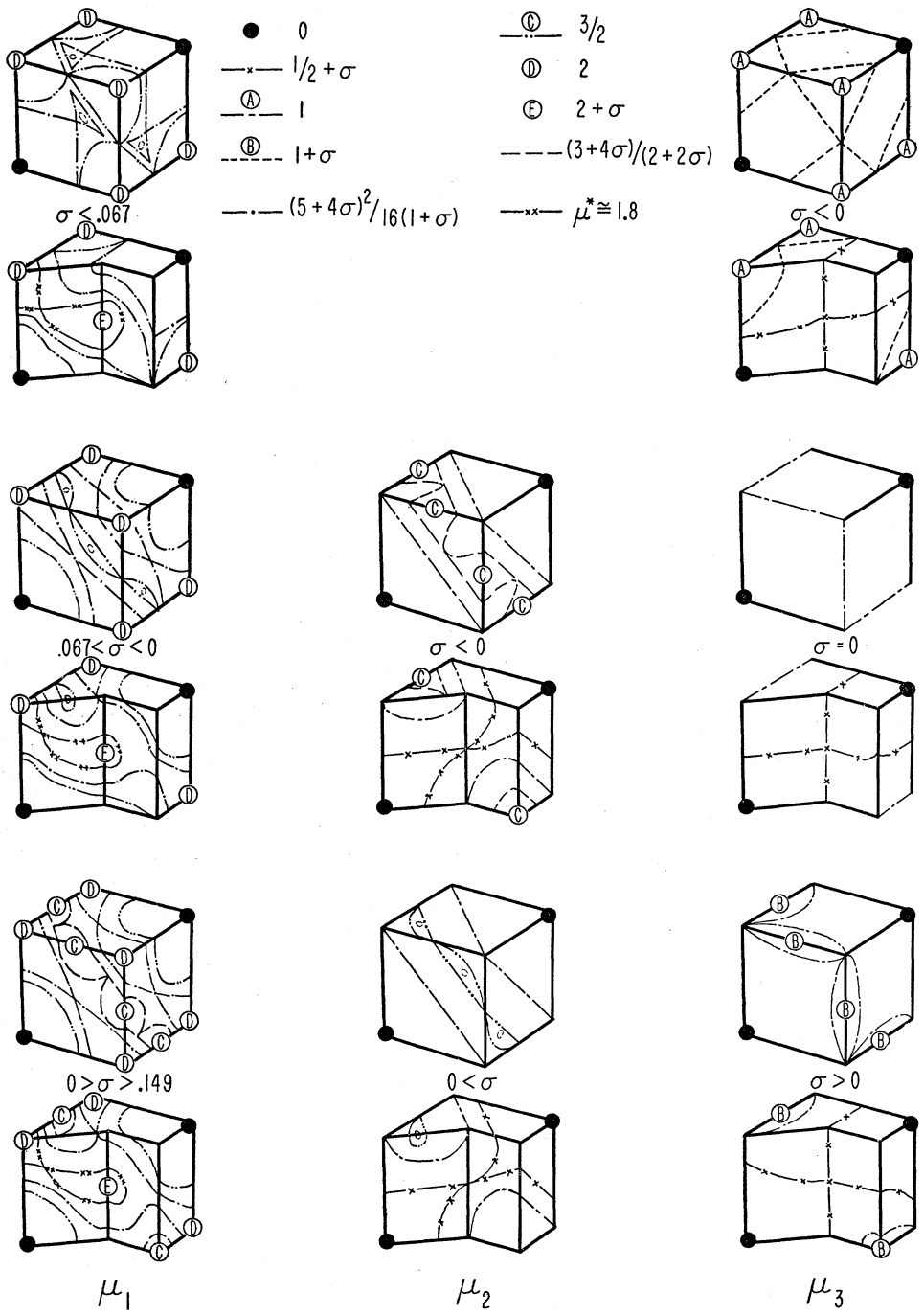

FIG. 9. Sketches of surfaces of constant frequency, face-centered cubic lattice.

shown on the surfaces of the drawings of Fig. 9 are obtained for $\sigma<\sigma^+$. Since in contrast to the other lattices considered in this paper, the fcc is not unstable for all $\sigma<0$, we include sketches of solutions for $\sigma<0$ whenever they are different from the ones for $\sigma>0$. Along the main diagonal inside the cube, each solution is found to have a CP at the origin. In two cases $\mu=\frac{1}{2}+\sigma$ and the CP is a S_3 for $\sigma<\frac{1}{6}$, in the third case $\mu=2+\sigma$ and the CP is a M_3 for all σ. This gives a consistent interpretation for the solutions μ_2 and μ_3, but the fact, revealed by expanding, that μ_1 is smaller than 2 in the neighborhood inside the cube of the points $(1, 1, -1)$ indicates that another S_3 point must exist inside the cube. This point is not located on the diagonal that runs from (0,0,0) to $(1, 1, -1)$ and so we have not been able to locate it or find the exact frequency μ^* of the critical

surface. However for $\sigma=0$ the minimum value of μ_1 along the diagonal $c_1=c_2=-c_3$ is $\mu_0=6(16+3\sqrt{2})/17 \cong 1.79$ and this value is not very sensitive to changes in σ; we may therefore conclude that $1.7<\mu^*<(2$ or $2+\sigma$, whichever is smaller). The final results are shown[26] in Fig. 9 and Table VII.

V. THE FREQUENCY DISTRIBUTION

The FD for the sc, bcc, and fcc lattices can be sketched directly from the information given in Tables V, VI, VII with the help of Table I. The sketches are given in Figs. 10, 11, and 12 respectively. The square lattice which has been rather fully treated by Montroll[6] has been included in this paper primarily to illustrate the problems in a simple way and will not be treated further. It is interesting to note in Fig. 10 that all new singularities that appear as ρ increases "grow out of" old singularities; this may be seen from Fig. 7 to be due to the fact that new CP invariably enter the cube by way of, or form out of, old CP. When we get a continuous surface of CP for the sc lattice (Fig. 7) and an inverse-square-root singularity, which is the singularity characteristic of 1D problems, appears in the FD. Physically this is due to the fact that, with nearest-neighbor interaction only, the motion in the x-direction of an atom in a sc lattice is independent of all atoms other than those in the x-direction, so that we are in effect dealing with a 1D problem. Similarly when $\sigma=0$ we get a continuous line of CP for the bcc and fcc lattice (Figs. 8 and 9, respectively) and a logarithmic singularity, which is the singularity characteristic of 2D problems, appears in the FD. For this we know no explanation as simple as for the inverse square root singularity in the sc lattice.

The only previous work that we can compare our results with nontrivially is Leighton's[16] numerical-mechanical computation of the fcc FD for two values of σ. Figure 13 shows Leighton's results for $\sigma=-0.1$ (replotted so that the abscissa is μ rather than $\mu^{\frac{1}{2}}$) together with the singularities found in this paper. Agreement is good; some of the singularities actually show up as discontinuities in the slope, though not as infinite ones (1,1.47), and others (0.4,0.9,λ^*,1.8) as rather sharp, though not discontinuous changes in the slope; some are slightly displaced. Clearly such smoothing would be expected to result from any numerical treatment. The agreement for $\sigma=0$ (not shown in Fig. 13) is equally good. The peak at $\mu=1$ is definitely there, though of course not infinitely high.

We cannot compare our work of that of Fine[26] since his choice of $\gamma=1$ falls outside our range. Our results

[26] The structure of μ_3 and μ_2 is comparatively easy to visualize. The essential surface is the one that goes through the S_3 point (0,0,0). The change in the surface of μ_3 as σ goes through 0 results from the fact that $1+\sigma \gtrless 1$ as $\sigma \gtrless 0$. The structure of μ_1 is somewhat similar to μ_1 and μ_3 in the bcc lattice (see reference 25): The surface $\mu=\mu^*$ consists of a closed surface which encloses the origin and to which six cup-shaped appendages are attached.

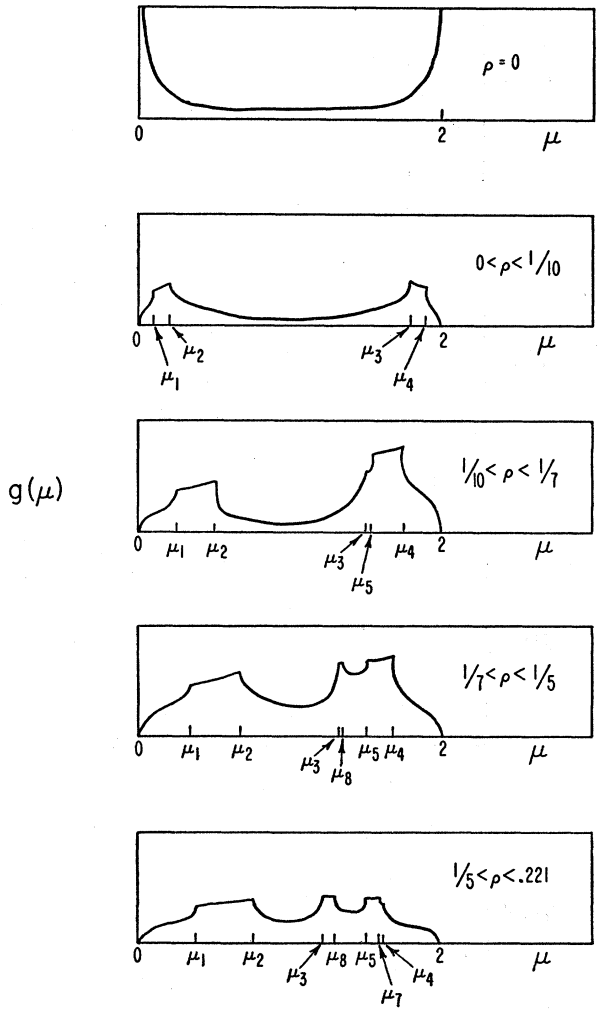

FIG. 10. Sketches of frequency distribution, simple cubic lattice.

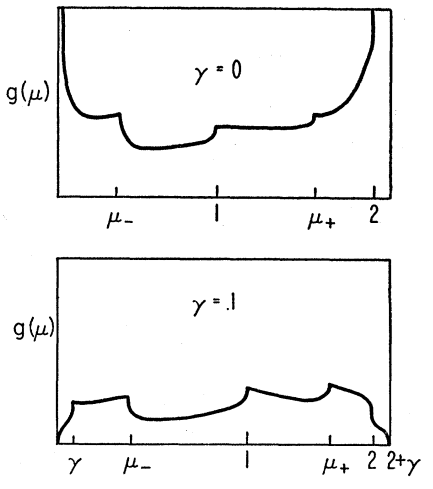

FIG. 11. Sketches of frequency distribution, body-centered cubic lattice.

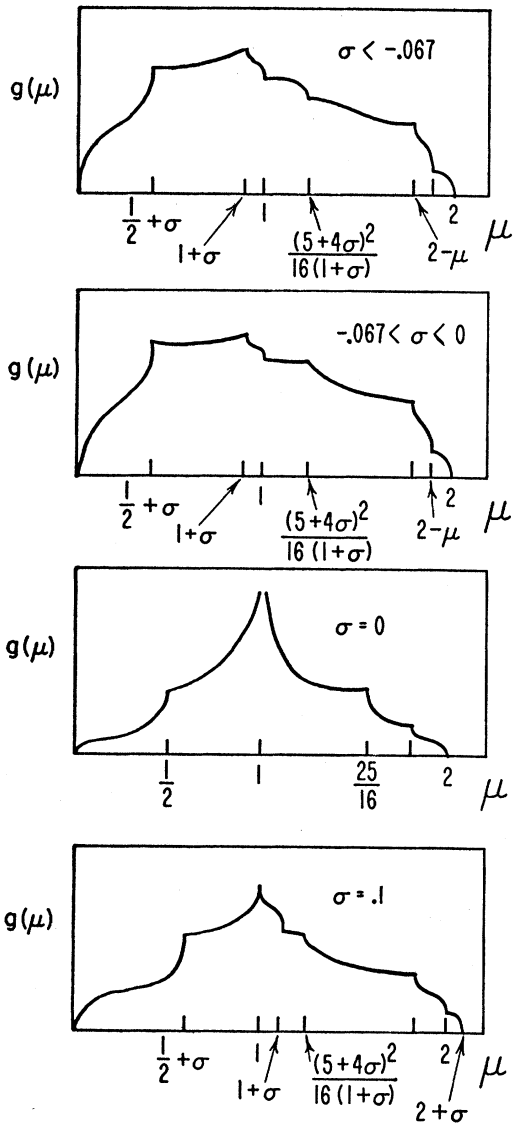

FIG. 12. Sketches of frequency distribution, face-centered cubic lattice.

are in agreement with Montroll's[6] for the square lattice and Newell's[9] for the simple cubic lattice for small ρ, as they must be since Montroll's and Newell's calculations are exact. Our results do not agree with Bauer's[27] who obtained many infinite peaks in his FD for the body-centered cubic lattice. This may be attributed to Bauer's use of Houston's[28] approximation.

[27] E. Bauer, Phys. Rev. **92**, 58 (1953).

[28] W. V. Houston, Revs. Modern Phys. **20**, 161 (1948). The idea on which the approximation is based is the replacement of the integration over the cube $0<x_1, x_2, x_3<\pi$ in the exact expression

$$g(\omega^2)=\int\int\int\delta[\omega^2-F(x_1x_2x_3)]dx_1dx_2dx_3$$
$$=\int\int\int\delta(\omega^2-F)r^2dr\,\sin\theta d\theta d\phi,$$

where $\omega^2=F(x_1x_2x_3)$ is the expression for ω^2, by a sum $\sum_n c_n\int\delta(\omega^2-F)r^2dr$ over a finite number of directions (ϕ_n,θ_n), and interpolating and normalizing properly. What makes the approximation useful is the fact that for certain directions (ϕ_n,θ_n) the expression $\omega^2=F$ is simple enough for the r-integration to be carried out, whereas in general it is not. The concomitant difficulty is that these directions are the ones running from the origin to a corner; i.e., from and to a CP. As a result, the triple integration over the CP is in effect replaced by a single one, and the singularities that appear in the 3D FD are of the nature that is correctly obtained in the 1D case, that is to say, infinite peaks of inverse square root nature. The appearance of spurious infinite peaks in Houston's approximate method has been previously discussed in connection with two specific 2D problems in reference 8 and by T. Nakamura, Progr. Theoret. Phys. (Japan) **5**, 213 (1950). It should be said that Bauer seems to be aware of the shortcomings of the method.

VI. THE ABSOLUTE VALUE OF THE FD

In the foregoing we have, for certain lattices and force constant ratios, found the frequencies at which the FD has singularities and established the nature of each singularity. We have not, however, done anything to find the absolute value of the FD at any point, except trivially at the end points where $g=0$. In this section we indicate briefly an approximate method by which, once the position and nature of the singularities is known, the FD may be found quantitatively with what we believe to be little labor for the accuracy attained. One sample calculation which bears out this belief has been performed.

The idea is to modify Montroll's approximate method, which was discovered at a time when the existence of singularities in the FD was not known, in such a fashion as to take proper account of the singularities. This occurred simultaneously to Lax and Lebowitz[29] and the writer.[30] Montroll's original method[31] may be described thus: Expand the frequency distribution,

$$g(\lambda)=\sum_n p_n\phi_n(\lambda), \tag{24}$$

the $\phi_n(\lambda)$ being known functions, such as Legendre polynomials, powers of λ, etc.; the p_n are coefficients undetermined at this point. Multiply each side by λ^k and integrate over λ; the result is

$$m_k=\sum_n a_{kn}p_n, \tag{25}$$

where $m_k\equiv\int\lambda^k g(\lambda)d\lambda$, called the kth moment of the FD, is seen to be the average value of λ^k, and $a_{kn}=\int\lambda^k\phi_n(\lambda)d\lambda$ can be directly computed. If we knew the first s moments, we could cut the sum off at $n=s$ and solve the set of s equations (25) for the expansion coefficients p_n. Equation (24) would then give us the FD approximated by a linear combination of a finite number of the functions $\phi_n(\lambda)$. The point is that the average value of λ^k, which may also be written

$$m_k=\int\int\int\tfrac{1}{3}\sum_{i=1}^{3}\lambda_i^k dx_1dx_2dx_3, \tag{26}$$

[29] M. Lax and J. L. Lebowitz, Phys. Rev. **95**, 617(A) (1954); Phys. Rev. **96**, 594 (1954). Detailed calculations for one 2D crystal are given.

[30] See footnote to title.

[31] E. W. Montroll, J. Chem. Phys. **10**, 219 (1942).

may indeed be easily computed even when λ_i is not known explicitly; for (1) may be written as $M\psi=\lambda\psi$, where M is the matrix of the determinant Δ with λ set equal to 0; multiplication from the left by M^{k-1} gives $M^k\psi=\lambda^k\psi$. An elementary theorem of matrix algebra then states that

$$\mathrm{Tr}(M^k)=\sum_{i=1}^{3}\lambda_i{}^k;$$

hence from (26)

$$m_k=\int\int\int \tfrac{1}{3}\,\mathrm{Tr}(M^k)dx_1dx_2dx_3. \qquad (27)$$

To take account of the singularities we merely replace (24) by something like

$$g(\lambda)=\sum_{j=1}^{m}F_j(\lambda)1(\lambda_{j-1},\lambda_j), \qquad (28)$$

where

$$1(a,b)=\begin{cases}1 & a<\lambda<b\\ 0 & \text{otherwise,}\end{cases}$$

and $\lambda_0=0<\lambda_1<\lambda_2<\cdots<\lambda_m=\lambda_{\max}$ are the values of λ at which singularities in the FD occur, and F_j is a function which contains a number of undetermined coefficients and which has the correct behavior at λ_{j-1} and λ_j. The coefficients of the first term $|\lambda-\lambda_j|^{\frac{1}{2}}$ near any singularity can in principle be found by expansion of the determinant about the CP that causes the singularity; in practice this is easiest for Type-4 CP and most difficult for Type-1 CP on account of degeneracy; it may be easier to keep that coefficient undetermined.

The example we have treated is the sc lattice for $\rho=0.05$. The location and nature of singularities is found from Tables V and I. We assume the following f_j:

$$f_1=c_0+c_1\mu,$$
$$f_2=c_2+c_3\mu,$$
$$f_3=c_4(\lambda-0.1)^{\frac{1}{2}}+c_5(0.9-\lambda)^{\frac{1}{2}}+c_6,$$
$$f_4=c_7+c_8\mu,$$
$$f_5=c_9+c_{10}\mu.$$

That is to say, we took the additional shortcut of assuming that the FD was a straight line in the ranges (0,0.05) and (0.95,1) and ignoring the square-root-type singularities which appear at the end points of those ranges and which, according to the recipe given in the preceding paragraph, we should have taken into account. In the case at hand this is justified by the fact that the shortness of the range assures that these singularities will not affect the shape of the FD much. The total number of undetermined coefficients included was thus eleven; one of those, c_4, could be easily found from the determinant, and six more were eliminated by the use of the conditions that $g(0)=g(1)=0$ and that g is continuous for all μ; four simultaneous equations of the form (25) had therefore to be solved. The moments were taken from Montroll.[31] μ has been normalized to run from 0 to 1. The results are shown in Fig. 14, the singularities at 0, 0.05, 0.95, 1 having been restored. Newell's[9] exact FD is also shown. In view of the fair agreement obtained by the use of only four free parameters, it may be hoped that more complicated approximating functions, together with the use of a high-speed computer to solve the larger number of simultaneous equations, will give accurate results. We hope to present results of such calculations in the future.

I wish to thank Professor W. A. Bowers for discussions and criticism and Mrs. H. M. Rosenstock and Mr. I. H. Blifford for help with computations.

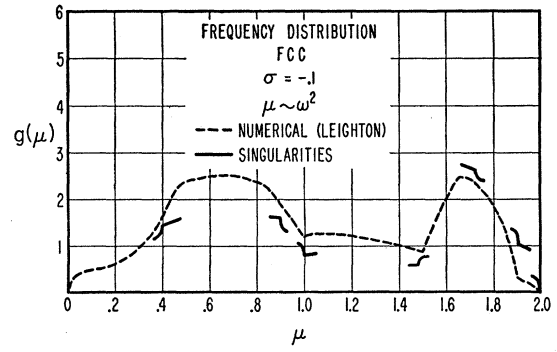

FIG. 13. Comparison between Leighton's numerical work and the results obtainable from this work for the square lattice.

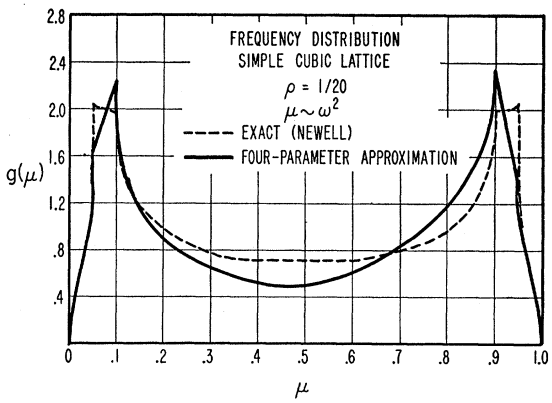

FIG. 14. Frequency distribution obtainable by applying Montroll's approximate method to the results of this work, compared with Newell's exact result for the simple cubic lattice, small ρ.